TESTS ON CONCRETE BEAMS REINFORCED WITH GLASS FIBRE REINFORCED PLASTIC BARS

Nebojša ĐURANOVIĆ[*1], Kypros PILAKOUTAS [*2] and Peter WALDRON[*3]

ABSTRACT: Results of tests on beams reinforced with steel and GFRP bars are presented. Three different approaches to design are examined by referring to the stiffness, area and strength of reinforcement. Analysis of experimental results shows that the classical approach of section analysis is valid and that predictable and repeatable results are obtained. The shear capacity of beam is also seen to be predictable, even though GFRP links have weaker characteristics than GFRP bars.
KEYWORDS: GFRP, beam testing, reinforced concrete, design, stiffness, flexure, shear

1 INTRODUCTION

Glass Fibre Reinforced Polymer (GFRP) reinforcement bars have mechanical and chemical characteristics which make them suitable for use in concrete construction, when corrosion of reinforcement is one of the main problems. However, before the adoption of any new reinforcement in construction extensive research is required to enable engineers to understand its fundamental behaviour and differences with conventional reinforcement.

This paper will present some of the experimental work undertaken at the University of Sheffield for the EUROCRETE project, which aims to develop FRP reinforcement for concrete. Failure loads and displacements are compared with the values calculated according to British Standard BS8110 [1].

2 EXPERIMENTAL DETAILS

Three phases of beam testing were undertaken for EUROCRETE. This paper will only consider the first phase. Reinforced concrete beams used for the tests had a rectangular cross-section 250mm x 150mm, overall length of 2.5m, span of 2.3m and were

[*1] Centre for Cement and Concrete, Dept. of Civil Eng., University of Sheffield, UK, Post-Doctoral Researcher.
[*2] Centre for Cement and Concrete, Manager, Dept. of Civil Eng., University of Sheffield, UK, Lecturer.
[*3] Centre for Cement and Concrete, Director, Dept. of Civil Eng., University of Sheffield, UK, Professor.

subjected to four point bending, as shown in Figure 1. All the beams were freely supported.

All the beams tested were made of concrete with a target compressive strength of 35 MPa and maximum aggregate size of 20mm. 13.5mm diameter GFRP rods manufactured for EUROCRETE were used as main reinforcement in all tests described. GFRP rods have a direct tensile strength of around 1000 MPa whilst the modulus of elasticity was obtained experimentally to be 45 GPa. Reinforcement links used for the beams were either made of high yield steel (characteristic tensile yield strength 460 MPa - experimentally measured 600 MPa, Young's modulus 200 GPa) or of the same GFRP material as the bars. GFRP links had a rectangular cross-section 10mm by 4mm, whilst steel links were made of 8mm diameter deformed steel bars. The GFRP links, produced by filament winding, have a flat smooth surface whilst GFRP bars, produced by pultrusion, have small shallow deformations. A typical reinforcement cage used in these tests is presented in Plate 1.

Plate 1 - GFRP reinforcement cage used for tests GB5, GB6, GB9 and GB10

Stresses measured by means of strain gauges on the GFRP closed-loop links never amounted to more than 270MPa, even in cases when the beam failed in shear due to link fracture. This indicates that the tensile strength of the links is much lower than the strength of the GFRP bars. This value is comparable to values obtained from tests conducted on isolated GFRP links in a specially designed rig that supported the link at the corners. The results from these tests showed a link strength of 390 - 410 MPa. Link failure always occurred at the corner.

The apparent reduction in the tensile strength of GFRP links when compared to the direct tensile strength of the material can be attributed to the geometry, material properties and manufacturing process. The links were made by winding-up continuous glass fibres around a wooden mould, so effectively producing a hollow rectangular section. After the removal of the wooden mould, this GFRP hollow section was cut into the desired link widths. The cutting process inevitably leads to a number of fibres being cut and thus reducing the effective area of the link. The loss of effective area is related to the angle at which the fibres were wound during manufacture. Continuous FRP elemants are inherently weaker in the direction perpendicular to the fibre than along the fibres. At the corners of links the geometry imposes a 90° change of direction of the force and stress. This can only be achieved through stresses perpendicular to the fibre direction. The magnitude of these stresses depends on the radius of curvature at the corner and the thickness of the link. For small radii of curvature, the lateral strain can be very high, leading to a massive loss of uniaxial tensile strength.

The beams of phase 1 were cast in groups of four and in Table 1 are shown in the groups in which they were cast. The beams that are not shown are not relevant for the purposes of this paper. In all the tests, apart from GB12, two point loading was applied at 767mm from the support, as shown in Figure 1. GB12 had the loads applied at 512mm from the supports. Table 1 presents the concrete and reinforcement details including the compressive (f_{cu}) and tensile (f_{ct}) strength of concrete; the number of main reinforcement bars (n) and the type of material (mat.), the cross-sectional area (A_{stir}) and the spacing (s_v) of the stirrups. Figure 1 shows a typical beam and the loading arrangement [2].

Table 1. - Concrete and reinforcement details

	Concrete		Bars		Stirrups	
Test No.	f_{cu} (MPa)	f_{ct} (MPa)	n	mat.	A_{stir} (mm”)	s_v (mm)
GB1	30.0	2.85	3	steel	50.3	153
GB2	38.1	2.94	3	---	---	---
GB5	31.2	2.78	3	GFRP	40	35
GB6	32.9	2.78	3	---	---	---
GB9	39.8	3.01	3	GFRP	40	76.7
GB10	39.8	3.01	3	GFRP	40	76.7
GB11	39.8	3.01	3	GFRP	40	153
GB12	39.8	3.01	3	GFRP	40	153
GB13	43.4	3.57	2	GFRP	40	76.7

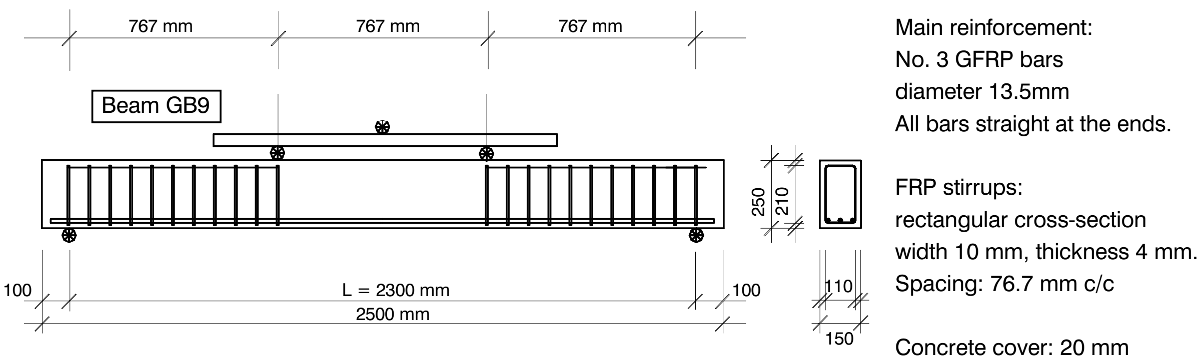

Figure 1 - Reinforcement and loading scheme for GB9

3 FLEXURAL DESIGN APPROACHES

Since the geometry of the specimens was similar, the main variable in the tests described is the type and amount of reinforcement. Steel reinforced reference beams are used in this section when exploring the various possible design approaches, substituting for the different types of reinforcement, such as equal stiffness, equal strength or equal area. These beams are designed and analysed without the use of safety factors. The concrete strength used was C40. The results are shown in Table 2 together with the results of the GFRP beams tested.

Table 2. Test and reference beams

Mater.	Design approach	Reinforcement Area (mm^2)	Percent. (%)	E A (kN x10^3)	Section capacity (kN)	Failure pattern	Neutral axis (mm)
GFRP	GB 1-12	429.4	**1.31**	**19.3**	**100.2**	**conc.**	**56.0**
steel	stiffness	96.6	0.94	19.3	32.1	reinf.	56.0
steel	strength	715.7	2.17	143.1	183.5	conc.	112.3
steel	area	429.4	1.31	85.8	126.0	reinf.	100.6
GFRP	GB 13	286.3	**0.87**	**12.9**	**85.5**	**conc.**	**47.0**
steel	stiffness	64.4	0.20	12.9	21.6	reinf.	47.0
steel	strength	477.1	1.45	95.4	137.4	reinf.	104.4
steel	area	286.3	0.87	57.2	88.8	reinf.	86.8

The stiffness approach requires that the reference and the GFRP beam are designed to have similar reinforcement stiffness. For beams reinforced according to this approach, serviceability limit state conditions such as deflections and crack width will be automatically satisfied. The area of GFRP reinforcement is significantly larger then the area of steel, by E_s/E_{GFRP}, and the cross-section will almost certainly be over-reinforced. This method does not lead to a significant shift in the position of the neutral axis between the reference and the GFRP beam and a massive increase in the ultimate capacity of the GFRP is achieved through the change of the failure pattern, i.e. reinforcement yield changes to concrete compressive failure.

The equal strength approach inevitably leads to a smaller amount of GFRP reinforcement and a significant reduction of the beam stiffness after initial concrete cracking. In all cases, the serviceability limit state conditions given for steel reinforced sections will be exceeded. Despite the significant reduction in the area of reinforcement this method will again, in general, produce over-reinforced sections, due to the lower elastic modulus of GFRP bars. In this case the change of the failure pattern may lead to a reduction in the ultimate capacity of the section. In both GFRP reinforced beams shown in Table 2, a reduction in capacity of around 40% is observed. In all cases the neutral axis will shift upwards and, consequently, concrete will become less utilised and the beam will have a lower stiffness.

The equal area approach leads again to a decrease in stiffness of the beam and a change of the mode of failure. This is as a direct consequence of the different tensile capacities, corresponding strains and, consequently, of the different level at which sections reinforced with GFRP and steel become balanced. Reference specimens reinforced only lightly will lead to GFRP equivalents with similar ultimate capacities, as GB 13, whilst for all other conditions this change will be negative, or negligible, as in the case of beams GB 1-12.

Obviously, the choice of design approach will depend on the design constraints. When stiffness is of paramount importance, such as when dealing with deflections, then more FRP reinforcement will be required than steel. However, in many applications, when strength is important, savings in the amount of reinforcement can be achieved.

4 TEST RESULTS AND CODE PREDICTIONS

Failure of beams in phase 1 resulted either due to concrete crushing compression or diagonal shear. Plate 2 and Figure 3 show results from the test on GB10 which failed in flexure, whilst Plate 3 and Figure 4 contain data from the test on GB11, which failed near its flexural capacity in shear [3].

Plate 2 - Beam GB10 - Flexural failure at midspan

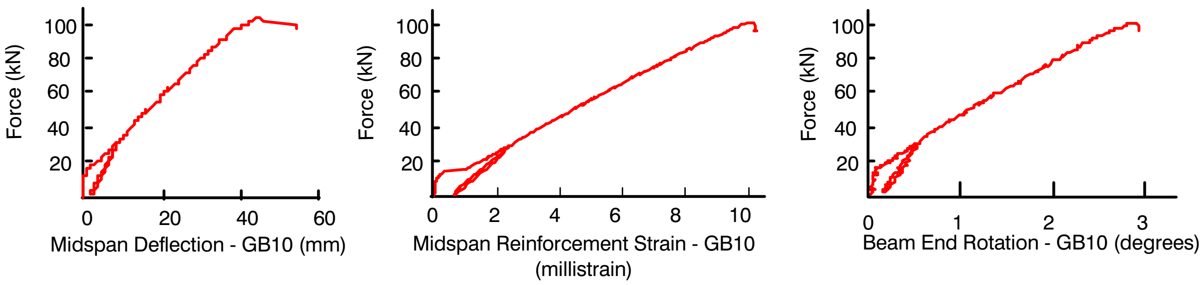

Fig 3 - Beam GB10 - Flexural failure at midspan

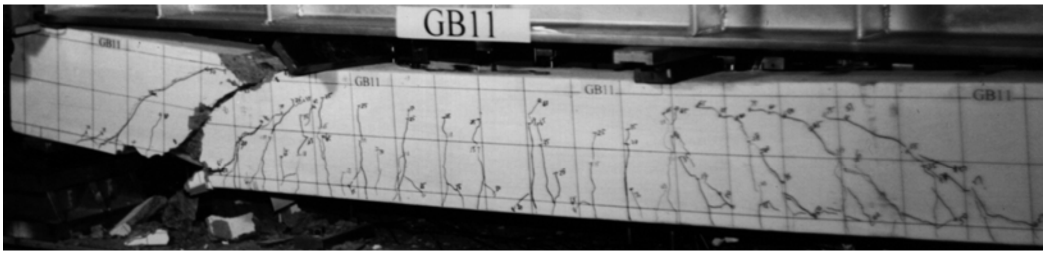

Plate 3 - Beam GB11 - Shear failure at support

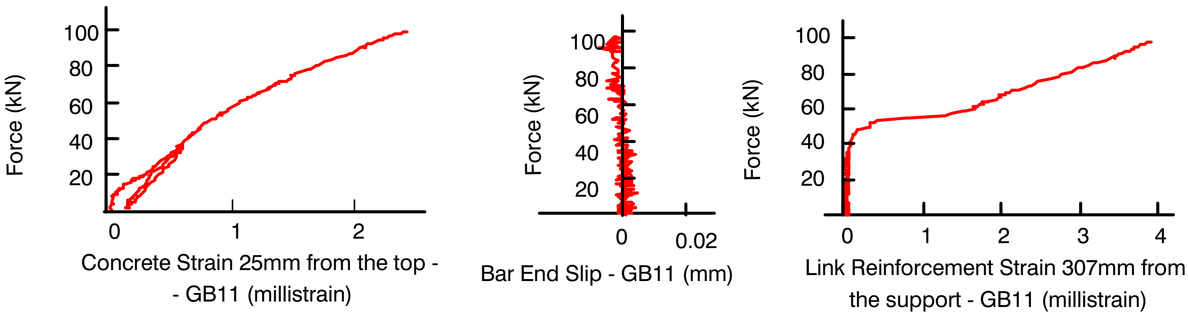

Fig. 4 Beam GB11 - Shear failure at support

One of the main reasons for conducting this initial work was to establish whether the procedure used for the analysis of steel reinforced sections could be used for sections with GFRP reinforcement. Table 3 shows the ultimate loads obtained experimentally and those calculated by using the sectional analysis approach, which assumes:

a. there is a linear distribution of strains along the height of the section, i.e. plane sections remain plane,

Table 3 - Comparison of analytical and experimental results

Beam No.	Analytical results P_{ult}(kN) (flexure)	Analytical results V_{ult}(kN) (shear)	Experimental results $P_{failure}$(kN)	Experimental results Failure mode
GB1	**82.9**	175.3	**97,8**	flexure
GB2	95.58	**46.2**	**52,9**	shear
GB5	**84.86**	156.0	**105,1**	flexure
GB6	97.1	**44.0**	**43,9**	shear
GB9	**98.1**	98.3	**103,6**	flexure
GB10	**98.1**	98.3	**103,0**	flexure
GB11	98.1	**72.67**	**97,95**	**shear**
GB12	146.9	**72.67**	**133,1**	shear
GB13	**88.1**	93.6	**90,6**	flexure

b. the stress distribution in concrete is as given by BS 8110 [4], without the material safety factors,
c. the tensile capacity of concrete can be neglected,

d. the reinforcement stresses are obtained from its pure tension stress-strain curve.
e. there is no bond slip between concrete and reinforcement.

5 DISCUSSION

It is clearly very difficult to show any significant amount of experimental data in such a paper, hence, the graphs presented were selected to demonstrate the potential of the information gathered during the testing programme.

Figure 3 shows deflections, strains and end rotations versus the applied load. It is very clear that the beam behaves in almost a bilinear manner with an initial stiffness to first cracking and then a second stiffness up to failure. The beam is quite deformable and the maximum mid-span deflection is comparable with deflections obtained at failure by steel reinforced beams. This is not surprising since the strain in the reinforcement at that stage is of the order of 1% as shown in the figure. The equivalent stiffness of normal steel bars (say 460MPa) at that strain is 46kN, which is the same as for the GFRP bars.

All GFRP beams of phase 1 which did not fail in shear failed by concrete crushing in compression. Large concrete strains can be seen in Figure 4. These were measured near the top of the beam by linear extension potentiometers, about 25mm below the top fibre. Since the neutral axis depth is very low, around 50mm, the strains recorded go beyond the strains at which we normally expect the concrete to fail. End slip displacements, shown in Figure 4, were used to determine bond failure, something that did not occur in any of the beams presented here. Strain measurements taken along the depth of the beam also helped to validate the assumption that plane sections remain plane.

Three beams unreinforced in shear failed at loads close to the predicted values as calculated by using modifications to BS8110 proposed by Clarke [5]. Beam GB 12 reinforced with GFRP links and designed to fail in shear did so, but at a substantially higher load than expected. Strains on the shear reinforcement exceeded values similar to those shown in Figure 4, but did not reach high stresses as discussed in section 2.

In fact, GB11 failed as a result of link fracture, just as the beam was reaching its flexural capacity, as seen from table 3. In this beam the link spacing was chosen in violation of the modifications proposed by Clarke [5] which only allow the development of a strain of 0.0025 on the shear reinforcement and lead to conservative design similar to GB5.

The results from the current project were reasonably consistent, proving the reliability of the given strength and stiffness of the bars used. This is clearly demonstrated by beams GB9 and GB10, tested under identical conditions. They both reached the same flexural load at the same central displacement of 45.4mm and cracking at loads of 13.7 and 14.5kN.

6 CONCLUSIONS

1) The behaviour of beams reinforced with GFRP bars has been shown to be predictable by section analysis techniques normally used in design.
2) The behaviour of the beams is reliable and repeatable. The deformability of beams at failure is similar to that of steel reinforced beams.
3) Different approaches for design are discussed and illustrated with examples. The choice of design approach depends largely on the design constraints.
4) Shear capacity is predictable by using modifications to equations proposed by Clarke. However, the strength of GFRP links appears to be limited due to a number of factors.

ACKNOWLEDGEMENT

Partners: Euro-Projects (LTTC) Ltd., Laing Technology Group, Sir William Halcrow and Partners Ltd., University of Sheffield, Allied Steel and Wire, Techbuild Composites Ltd., Vetrotex, DSM Resins, Statoil, Norsk Hydro and SINTEF. UK Funding Body: DTI/EPSRC, LINK Structural Composites Programme, NL Funding body SENTER. Associates: Tarmac Precast. Additional materials: Zoltek and Toray. The project has been granted EUREKA status and the assistance is acknowledged.

REFERENCES

[1] BS8110 - "Structural use of Concrete", British Standards Institution, 1985

[2] Duranovic, N., Pilakoutas, K. and Waldron, P., "General Testing Arrangements for R.C. Beams", EUROCRETE Rep. CCC/95/17A, Univ. of Sheffield, Feb. 1995, pp 4

[3] Duranovic, N., Pilakoutas, K. and Waldron, P., "General Testing Arrangements for R.C. Beams", EUROCRETE , CCC/95/21A, Univ. of Sheffield, Feb. 1995, pp 26-35

[4] Kong, F.K. and Evans, R. H., "Reinforced and Prestressed Concrete", Van Nostrand Reinhold (UK), London, 1987, pp. 70

[5] Clarke, J.L, O'Regan, D.P. and Thirugnanenedran, C., "Modification of Design Rules to Incorporate Non-Ferrous Reinforcement", Interim Report to EUROCRETE, Sir William Halcrow & Partners, London, September 1996.